Energy Conversion and Management 227 (2021) 113586

Contents lists available at ScienceDirect

Energy Conversion and Management

journal homepage: www.elsevier.com/locate/enconman

Selection optimization of variable speed pump as turbine (PAT) for energy recovery and pressure management

Shahin Ebrahimi [a], Alireza Riasi [a,*], Ali Kandi [b]

[a] Marine and Hydrokinetic Energy Laboratory, School of Mechanical Engineering, College of Engineering, University of Tehran, Tehran, 11155-4563, Iran
[b] School of Mechanical Engineering, Iran University of Science & Technology, Narmak, Tehran, Iran

ARTICLE INFO

Keywords:
Pump as turbine (PAT)
Water distribution network (WDN)
Pressure reducing valve
Energy recovery
Particle swarm optimization (PSO)

ABSTRACT

Renewable energy technologies around the world have become a priority today and among them, hydropower plants have the largest share. The most significant problem with small hydropower plants is the high cost of commercial turbines. The most economical way to generate small-scale energy is to use a pump as turbine (PAT) due to the cheapness and availability of the pump. In water distribution networks (WDNs), the PATs can be used instead of pressure reducing valves (PRVs) for both pressure reduction and energy production. The installed PAT must be capable of operating under different discharges due to fluctuations in rate of water consumption, which makes it challenging to select the appropriate pump. In this study, the process of PATs selection for PRVs replacement is optimized using particle swarm optimization (PSO) algorithm. Three different scenarios are performed for the optimization process, considering constant and variable speed PATs. It is worth mentioning that the wasted energy in the selected case study is about 494 kWh/day using PRVs. The results show, in scenario no. 3 (variable speed PATs), the total amount of produced energy is 182.15 kWh/day. Also, the penalty function is decreased by about 62% in comparison to other scenarios and as a result, the pressure of the critical nodes has better agreement to those values of PRVs utilization.

1. Introduction

Energy has always been one of the main and most important factors in the economic and social development of societies [1]. Throughout history, human beings have used various forms of energy to meet their needs [2]. Electricity, as the most practical type of energy, plays a key and vital role in today's human life, without which human life faces many problems [3]. The need for electricity in the world is expanding and will keep increasing with a high rate to 2050 [4]. In this regard, Fossil fuels have always been one of the common sources of power generation over the years [5]. However, due to some problems such as limited resources and environmental pollution that they cause in recent years, researchers and the engineers have focused on various types of renewable energies such as solar, hydropower, wind energy, etc. [6–8]. Benefiting renewable resources improves air quality and prevents further greenhouse gas emissions [9]. Besides, several agreements such as Paris and Montreal protocols have been ordained to reduce environmental effects as much as possible [10,11]. Hydropower is of particular importance because it accounts for 92% of all renewable energy production and 16% of all electricity produced worldwide [12].

Micro and Pico hydropower plants are of great interest due to issues of electrification in places without any access to the national grid [13]. However, the installation of hydropower plants less than 500 kW has high cost-per-kW due to the cost of electromechanical equipment (such as turbine and generator) and their maintenance [14]. Since pumps are mass-produced in various sizes and available at reasonable prices, their use in reverse operation can be a good alternative to conventional turbines [15]. Therefore, over the past years, extensive studies have been conducted by researchers on the turbine operation of pumps.

The idea of using pump as turbine was introduced in the mid-20th century, when Thoma, in an effort to achieve complete pump curves, accidentally realized that pumps could work as efficient turbines [16]. The main challenge of employing PAT is the unavailability of comprehensive descriptive relationships of its characteristic curves. Many researchers have used various methods to achieve relationships for predicting the performance of pumps in reverse. Chapallaz et al. experimentally obtained the conversion factors used to calculate the turbine mode characteristics of pumps [17]. Pascoa et al. performed a numerical and experimental study on an industrial pump in both direct and reverse modes. Considering their report, the operating efficiency in turbine mode is 4.4% less than pump mode [18]. Derakhshan and

* Corresponding author.
E-mail address: ariasi@ut.ac.ir (A. Riasi).

https://doi.org/10.1016/j.enconman.2020.113586
Received 1 July 2020; Received in revised form 19 October 2020; Accepted 20 October 2020
Available online 9 November 2020

Nomenclature

c_1	Personal learning coefficient (–)
c_2	Global learning coefficient (–)
C_{HW}	Hazen-Williams coefficient (–)
D	Diameter (m)
g	Gravity acceleration (m/s^2)
H	Head (m)
$H_{BEP,T}$	Head of turbine at best efficiency point (m)
$H_{L,N}$	Head at runaway curve (m)
H_T	Head of turbine (m)
K	Leakage factor (L/s.m$^{0.5}$)
L	Length (m)
n	Rotational speed (rad/s)
$P_{i,\ j\ (PAT)}$	Pressure of node j at time i, in PAT operation (m)
$P_{i,\ j\ (PRV)}$	Pressure of the node j at time i, in PRV operation (m)
P_{j1}	pressure of node j before installing PAT (m)
P_{j2}	Pressure of node j after installing PAT (m)
Pen	Penalty function ($)
Q	Flow rate (m^3/s)
$Q_{BEP,T}$	Flow rate of PAT at best efficiency point (m^3/s)
$Q_{L,N}$	Flow rate at runaway curve (m^3/s)
Q_T	Flow rate of turbine (m^3/s)
R	Pipe resistance constant (s$^{1.852}$/m$^{4.556}$)
t_a	Water tariff ($/m^3)
t_e	Energy tariff ($/kWh)

Greek letters

α	Penalty coefficient ($/m)
η	Efficiency (–)
$\eta_{BEP,P}$	Efficiency of pump at best efficiency point (–)
$\eta_{BEP,T}$	Efficiency of turbine at best efficiency point (–)
φ	Non-dimensional flow (–)
ψ	Non-dimensional head (–)
ω	Inertial coefficient (–)

Nourbakhsh studied four centrifugal pumps at specific speeds of less than 60 in both direct and reverse modes. The outcomes of their study revealed that by increasing the specific speed, the ratio of head and discharge at the BEP of the turbine to the same values of the pump will decrease [19]. Derakhshan and Nourbakhsh presented a theoretical method for calculating the best operating point of a PAT based on its direct mode characteristics. According to this method, the numerical results are quite different from the experiments due to the lack of casing modeling that neglects any leakage between the impeller and the volute [20].

Barbarelli et al. used a numerical model to predict centrifugal pump performance in turbine mode using only the information contained in the pump catalog. They also experimentally obtained the characteristic curves of 6 centrifugal pumps with a specific speed of 9–65 in turbine mode and compared them with the mentioned numerical method [21]. In an experimental and numerical study, Barbarelli et al. determined a method for selecting appropriate PAT according to site characteristics. The method proposed by them modified the pump selection by evaluating the efficiency at the point of operation of the power plant [22].

One of the new ideas in the field of PAT is to use them as PRVs in WDNs. Due to the topography of the cities, the water pressure rises inside the pipes, which a PRV adjusts the excess pressure inside the transmission lines to prevent breakage and manage the pressure of the network. But nowadays, it is possible to extract electricity from water transmission lines using water turbines or PATs. Investigating the methods of selecting the appropriate PAT in order to make the best use of the hydropower plant, given the operational complexities of the network, is one of the topics of interest to researchers. In the variable operating strategy developed by Carravetta et al., A model is proposed to select the appropriate PAT for the WDN considering the hydraulic characteristics of the pressure reducing station and a method to help the energy recovery system for regulating network pressure [23]. Jian Do et al. investigated the performance of PAT for use in Hong Kong's high-rise building water supply system numerically and empirically. The results of both numerical and experimental studies indicate the feasibility of using PAT to reduce excess head and generate power [24].

In a study, Fontana et al. studied the energy recovery of PAT at a constant speed and its use in replacing PRV. Using a genetic algorithm, searched for PAT optimal location in the network. Avoiding of wasting a large amount of water along with recovering a significant amount of power was reported by them, although their chosen objective function was not to maximize the energy produced [25]. Tahani et al. conducted an experimental study on the performance of variable speed PAT in the water distribution network. They provided relationships for describing PAT performance curves in the case of large speed variations and emphasized on the need for research in its application [26].

Tracy Lydon et al. investigated the selection of appropriate constant speed PATs for replacing PRVs in the WDN of Dublin numerically and concluded that using PAT could recover up to 40% of the hydraulic potential lost by PRVs [27]. Lima et al. developed an innovative method for selecting constant speed PAT and locating it to replace the PRV within the network. Their method was based on maximizing the produced power and reducing leakage due to system pressure constraints. They, with emphasis on hydraulic changes in the water network, stated that PAT and PRV performance were the same at peak consumption times, but at low discharges, PAT performance was impaired and could not provide desired output pressure [28]. Alberizzi et al. simulated the performance of PAT at the inlet of the WDN and studied the ability of pressure management. Using an averaged flow rate, they investigated the possibility of creating the desired downstream pressure with the aim of maintaining PAT performance near the BEP during discharge fluctuations. They reported the use of PAT speed variation as a suitable solution to use all available discharges [29].

Despite various studies on the use of PAT as a PRV, the impact of using variable speed PAT as a PRV for energy recovery has been less investigated. In this study, the selection of a suitable combination of variable speed PATs for replacement with PRVs in the WDN is optimized using PSO algorithm. The optimization process is performed in 3 different modes. In the first stage, the rotational speed of all PATs is considered to be the same and constant. In the second stage, PATs can have different rotational speeds, but this speed is constant during the day, in other words, in addition to selecting the optimal PATs, their optimal operating speed is also obtained. In the third stage, PATs can have different rotational speeds, but the speed of PATs is not constant during the day and PATs can have speed variation, and in addition to selecting the optimal PATs, their optimum operating speed has also been obtained during the operation. For this purpose, the turbine mode performance curves of existing industrial pumps for a wide range of specific speeds have been extracted using the methods presented in [30,17]. The desired network is simulated by considering the selected PATs and the harvested energy, as well as the pressure of critical nodes, were calculated. The results of optimizing the performance of the variable speed reverse pump firstly give a more clear understanding of how the system operates in controlling the pressure and its effect on the network. In addition, the positive effects of optimizing speed variation for improving the performance of the system will be accompanied by more production capacity and consequently higher revenue for the power plant.

2. Governing equations of the WDN

The governing equations used in the hydraulic analysis of networks are the relation of the flow continuity in the nodes and the relation of the loop head drop. The relation of the flow continuity of the nodes is expressed as Eq. (1) [31]:

$$\sum_{x_j} Q_x + q_j = 0 \quad (j = 1, 2, ..., n) \tag{1}$$

where q_j is demand at junction j and Q_x is the discharge of each pipe connecting to junction J. The relation of the loop head drop is also given by Eq. (2) [31]:

$$\sum_{x \in c} h_{Lx} = \Sigma R_x Q_x^n = 0 \quad (c = 1, 2, ..., C) \tag{2}$$

where $\sum_{x \in c} h_{Lx}$ describes the summation of the head loss along loop c. In this relation, R_x represents the pipe resistance constant. Hazen-Williams relation was used to obtain the pipe head loss and the R_x value was obtained from Eq. (3) [31]:

$$R = \frac{10.68L}{C_{HW}^{1.852} D^{4.87}} \tag{3}$$

In this equation, L describes the pipe length, D is the pipe diameter, and C_{HW} is the pipe's Hazen-Williams coefficient, which depends on the material of the pipe and its diameter. The equations of ΔQ method was applied for the hydraulic analysis of the WDN. Using this method, the relation of the loop head drop (Eq. (2)) is as follows [31]:

$$\sum_c R_x \left(Q_{1(x)} + \sum_x \Delta Q_c \right)^n = 0 \quad (c = 1, 2, ..., C) \tag{4}$$

where Σ_c represents the summation of head drop along loop c and Σ_x denotes the summation of the all corrective discharges pass through pipe x. After obtaining the governing equations of the network, the Hardy-Cross method is employed to solve them. The general form of the hardy-cross relation to calculate the ΔQ of loop c in the t-iteration is as follows [31]:

$$\Delta Q_{(t)c} = -\frac{\sum_{x \in c} R_x Q_{(t)x}^n}{\sum_{x \in c} n.R_x \left| Q_{(t)x} \right|^{n-1}} \quad (c = 1, 2, ..., C) \tag{5}$$

The case study has been considered in this study is shown in Fig. 1. This network consists of two tanks to supply water and two pumps to create the flow and appropriate pressure in the network. Three PRVs are also located in the network for adjustment and preventing pressure increase in nodes 4 and 6 (which are at a lower elevation than other nodes and tanks). Table 1 reports the physical characteristics of the pipes,

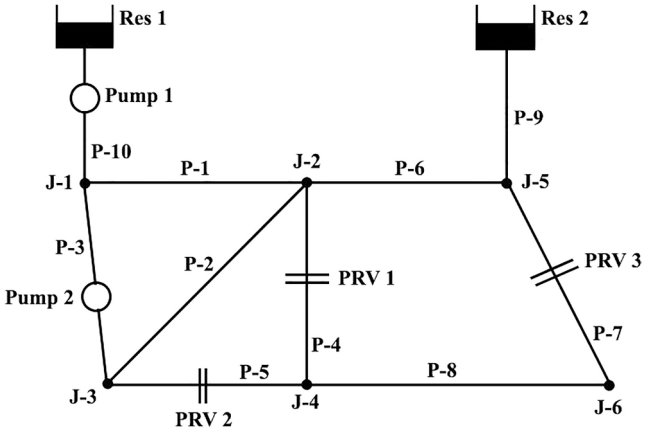

Fig. 1. Schematic of the considered WDN.

Table 1
Specifications of the considered WDN pipes(cast iron).

Pipe number	Diameter (mm)	Length (m)	Upstream node	Downstream node
1	152.4	609.6	1	2
2	152.4	609.6	2	3
3	152.4	762	1	3
4	203.2	518.2	2	4
5	152.4	243.8	3	4
6	152.4	304.8	5	2
7	203.2	914.4	5	6
8	152.4	1005.8	4	6
9	254	305	Res 2	5
10	254	305	Res 1	1

including the diameter and length of the pipes, as well as the upstream and downstream nodes of each pipe. It should be noted that the material of all pipes is cast iron.

Table 2 lists the information about the nodes in the studied network, including the elevation and flow rate of the average consumption as well as the elevation of the water supply (nodes 1 and 5 are the only the interface between the reservoirs and the rest of the nodes).

Table 3 reports the specifications of the pumps, both of which operate at 1450 rpm.

As mentioned, each network node has an average flow rate, but the actual flow rate of each node that changes during the day is obtained using the peak hour factor. Fig. 2 shows the peak hour factor hourly variation, which shows the network consumption pattern.

3. Modeling the performance curves of existing industrial pumps

A database is needed at first to perform the optimization operation. Industrial pumps used in water and wastewater applications have been utilized for this purpose. The turbine mode performance curves of existing industrial pumps for a wide range of specific speeds have been extracted considering the methods presented in Gulich [30] and Chapallaz [17].

The general relation presented by Gulich [30] for the turbine characteristic curve of a centrifugal pump is as:

$$H_T = H_{BEP,T} - \frac{H_{BEP,T} - H_{L,N}}{Q_{BEP,T}^2 - Q_{L,N}^2} \left(Q_{BEP,T}^2 - Q_T^2 \right) \tag{6}$$

The parameters in the above relation are obtained by using the available relationships [17,30]. Affinity law has been also applied to obtain PAT characteristics at the desired speed.

Fig. 3 shows the turbine performance curve of a pump with a specific speed of 23.8 at the rotational speed of 1500 rpm and 3000 rpm. According to this figure, it is determined that as the rotational speed of the PAT increases, its characteristic curve shifts upwards. In other words, at a certain flow rate, the value of the PAT output head increases with increasing rotational speed.

To validate the method, the above H-Q curve is converted to the non-dimensional curve using the following equations. Fig. 4 depicts the

Table 2
Nodes characteristics of the considered WDN.

Node number	Average demand (m^3/h)	Elevation (m)
1	0	122
2	133.8	122
3	51	106.7
4	25.5	18.3
5	0	122
6	25.5	18.3
Res 1	–	122
Res 2	–	152.5

Table 3
Characteristics of the pumps installed in the WDN.

	H (m)	Q (m^3/h)
Pump 1	33.5	152.9
	31.7	254.9
	28	356.75
Pump 2	4.57	152.9
	3.66	203.9
	2.3	305.8

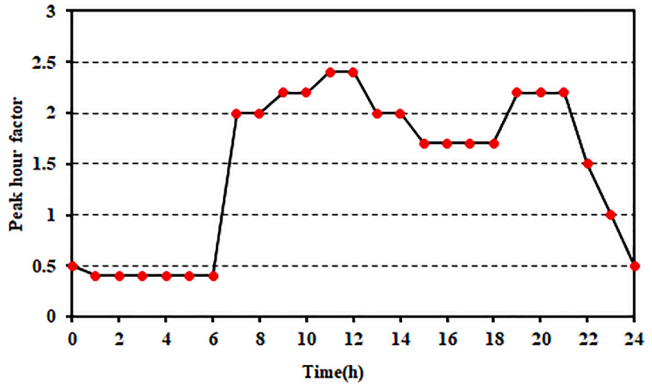

Fig. 2. Pattern of water consumption during a day.

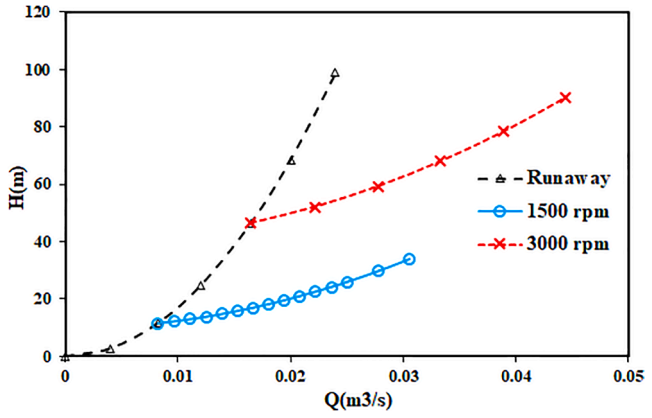

Fig. 3. *H-Q* diagram of a PAT with specific speed 0f 23.8 at two different rotational speeds.

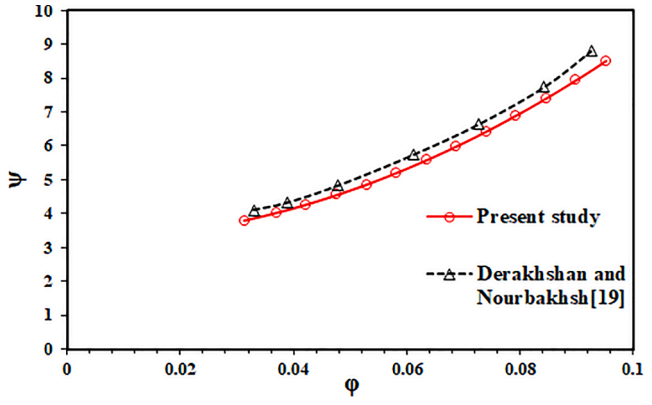

Fig. 4. Comparison of ψ-φ diagram.

comparison of this study and the experimental results of Derakhshan and Nourbakhsh [19]. According to the figure, it is clear that the curve obtained from the mentioned method is in acceptable agreement with the experimental data obtained by Derakhshan and Nourbakhsh [19].

$$\psi = \frac{gH}{n^2D^2} \tag{7}$$

$$\varphi = \frac{Q}{nD^3} \tag{8}$$

The η-Q curve of the turbine mode should be extracted. For this purpose, the graph presented by Gulich was applied and the efficiency at the BEP of PAT has been calculated by Eq. (9) [30]:

$$\eta_{BEP,T} = \eta_{BEP,P} - 0.03 \tag{9}$$

Also Fig. 5 illustrates the comparison of the obtained curve with the one reported by Derakhshan and Nourbakhsh [19].

4. PAT selection optimization

The main task of controlling the pressure through PAT, instead PRV, is to generate clean energy in the WDN, and since this parameter has a direct impact on the power plant economy, it is highly regarded. Another important issue in the network is water leakage, which is closely related to pressure management. Therefore, to select a suitable PAT for replacement with a PRV, both parameters must be considered. The constraints of the problem are also considered in the form of a penalty function. The objective function is as follows [28]:

$$FO = \sum_{i=1}^{24}\left[t_e.\frac{\gamma Q_i H_i \eta_i}{1000} + \sum_{j=1}^{n} t_a.K.\left(\sqrt{P_{j1}} - \sqrt{P_{j2}}\right)3600\right] - Pen \tag{10}$$

where:

FO [$]: The objective function to be maximized.
t_e [$/kWh]: energy tariff
Q_i [m^3/s]: PAT discharge in time i
H_i [m]: PAT head in time i
η_i: PAT efficiency in time i
n: nodes affected by PAT function
t_a [$/$m^3$]: water tariff
K [L/s.$m^{0.5}$]: Leakage factor
P_{j1} [m]: node j pressure in time i before installing PAT
P_{j2} [m]: node j pressure in time i after installing PAT
Pen [$]: Penalty function

The definition of a penalty function depends on the constraints. It is crucial to ensure that the pressure of all nodes have the same values when the PRV was used during 24 h. For this reason, the penalty function was defined as Eq. (11):

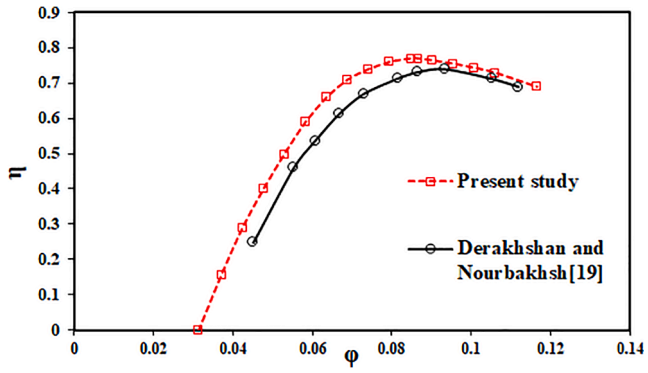

Fig. 5. Comparison of the efficiency curves.

$$Pen = \sum_{i=1}^{24} \sum_{j=1}^{n} \alpha . \left| P_{ij(PAT)} - P_{ij(PRV)} \right| \quad (11)$$

where:

α [$/m]: penalty coefficient
$P_{i,\ j\ (PAT)}$: Pressure of node j at time i, in PAT operation
$P_{i,\ j\ (PRV)}$: Pressure of the node j at time i, in PRV operation

PSO algorithm is employed to perform the optimization. This method is chosen because of its capability and easy implementation. This algorithm can be used to optimize a variety of issues including optimal design, pump scheduling, size and location determination of protective equipment installation [28,32]. In this algorithm, each particle has s dimensions. Parameter s describes the number of decision variables of the problem. The values of the decision variables determine the position of a solution in the optimization problem. Each i particle is determined by three vectors that are: the current position vector of particle $X_i=(x_{i1}, x_{i2},\ldots,x_{is})$, the best previous position vector of particle $B_i=(b_{i1},b_{i2},\ldots,b_{is})$ and the particle velocity $V_i=(v_{i1},v_{i2},\ldots,v_{is})$. In each iteration, the best position of the particle group is also determined and represented by the vector $G^*= (g_1,g_2,\ldots,g_s)$. In each iteration, after determining G *, the location of each particle of the group varies. This change is made by using Eq. (12):

$$X_i^{'} = X_i + V_i^{'} \quad (12)$$

The prime mark (′) indicates new values and the new velocity is obtained from the Eq. (13):

$$V_i^{'} = \omega V_i + c_1 rand_1(\,)(B_i - X_i) + c_2 rand_2(\,)(G^* - X_i) \quad (13)$$

here,

c_1: personal learning coefficient (leading the particle of the best-experienced value)
c_2: global learning coefficient (leading the particle of the best-experienced value by the group)
ω: Inertial coefficient (which indicates the capacity of the particle to remain on the current)
$rand_1$ () and $rand_2$ () are vectors with the length of the position vector, each of which is a random number between 0 and 1 with a uniform distribution.

In the optimization process, the decision variables were initialized and the network is modeled based on these values. After solving the network and obtaining its hydraulic values, the performance of the PAT was also calculated and determined. By calculating the cost function, which depends on the performance of PAT in power generation and reducing water leakage, it was compared with the convergence condition. If this condition is not satisfied, new values were given to the problem decision variables and this process continues until the convergence is established. The optimization was conducted for three different scenarios as shown in Fig. 6:

Using the algorithm in Fig. 6, three scenarios were investigated for optimization of PAT operation in the network including:

(a) *Scenario no. 1:* The rotational speed of PATs has been assumed constant during the day at 1450 rpm,
(b) *Scenario no. 2:* The rotational speed of each PAT is constant during a day but different to each other,
(c) *Scenario no. 3:* The rotational speed of each PAT could be independently variable during the day.

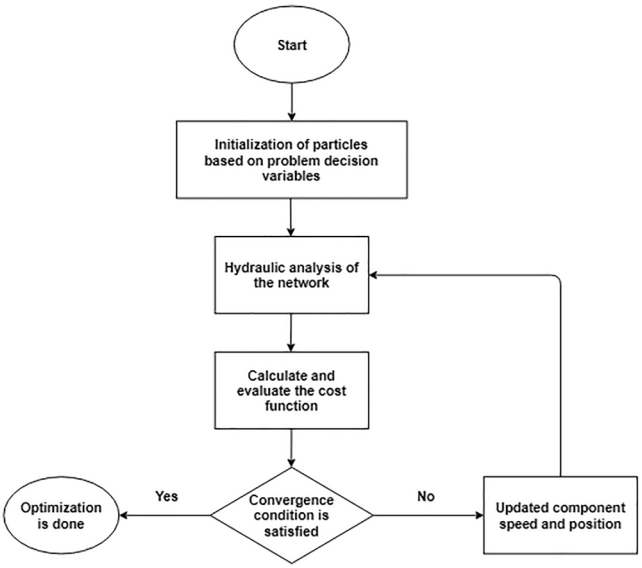

Fig. 6. Optimization algorithm.

5. Results and discussion

In this section the validation of the developed MATLAB code is shown and the results of the performed optimization are reported.

5.1. Validation

In order to verify the developed code in Matlab, the results of this code had been compared with those obtained by WaterCAD software at two critical nodes 4 and 6 in states of with using PRV, without using PRV and with using constant speed PAT, as shown in Figs. 7–9. As can be seen, there is a good agreement between the results of the code and WaterCAD in the calculated pressure values at different hours in both states of presence and absence of PRV. Due to the fact that WaterCAD has no function programming capability, it is not possible to simulate the state that the speed of PATs varies with time. So, the network with constant speed PAT mode is simulated with MATLAB and the results are validated with WaterCAD.

5.2. Scenario no. 1

The result of the performed optimization at this step is as follows. Three PATs were selected to replace with PRVs based on the hydraulic parameters. In Fig. 10, changes in objective function are shown in terms of iterations.

The obtained head and flow rate of the PATs was reported in Table 4. It should be mentioned that, BEP parameter of selected PAT are reported in rotational speed of 1450 rpm.

Fig. 11 shows the power output of each of these PATs, as well as the total power output of this combination within 24 h. The total power generated from the plant over 24 h is 152.4 kWh.

It can be seen from Fig. 10 that the output power of PAT no. 3 is zero during the period of 1–6 h and 23–24 h, which is due to the fact that the direction of the flow in pipe no. 7 reverses at these hours and as a result, the PAT acts as a check valve, preventing the flow of water in the opposite direction and thus the pipe flow was considered to be zero at these hours. Also, the power output of PAT no. 3 is much higher than the other two PATs from 7 to 22 h. Figs. 12 and 13 illustrate the pressure diagrams of nodes 4 and 6 during 24 h for three cases: uncontrolled network (no PRV), network with PRV and network with optimized PATs.

It is clear from the above figures that PAT performance is close to PRV when the network consumption is high, but by reducing network

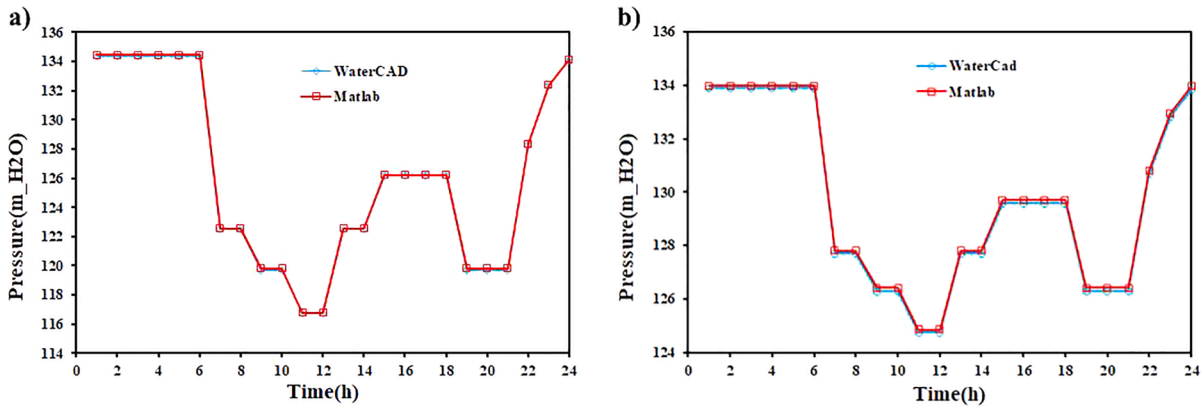

Fig. 7. Pressure of nodes a) 4 and b) 6, without using PRV.

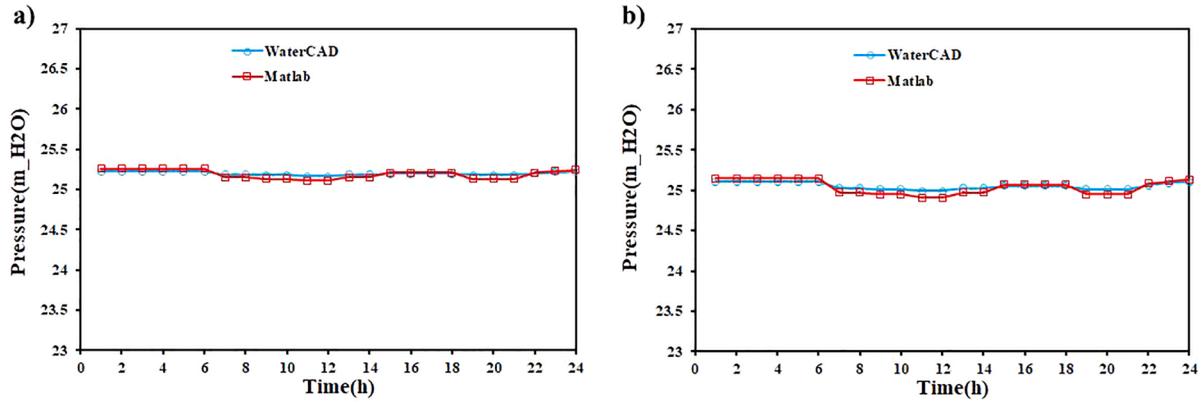

Fig. 8. Pressure of node a) 4 and b) 6, while using PRV.

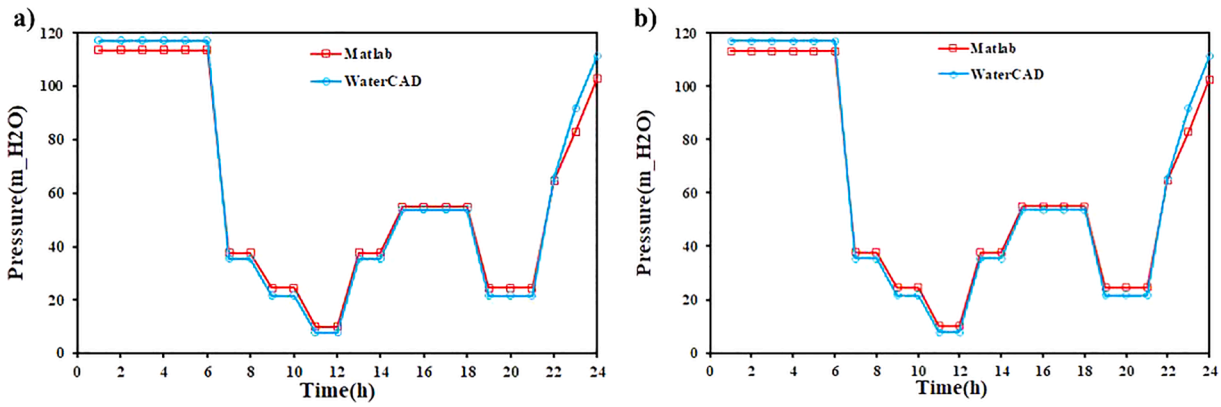

Fig. 9. Pressure of nodes a) 4 and b) 6, without using constant speed PAT.

consumption in the early and late hours of the day PAT performance shifts away from PRV, thereby the pressure of the nodes was increased above the desired.

5.3. Scenario no. 2

At this stage of optimization, the goal is to obtain the optimum speed of each PAT in addition to obtaining the optimal combination of PATs to replace PRVs in the network. The performance speed of PATs varies between 500 and 2800 rpm. Fig. 14 shows the FO value variation with iterations.

The head and the flow rate of the selected PATs in 1450 rpm and their optimum rotational speed were as reported in Table 5:

The total generated energy during 24 h is 196.92 kWh which is increased by 29.2% in comparison with the scenario no. 1. Fig. 15 shows the power output of each of these PATs, as well as the total power output of the combination within 24 h.

It can be seen from the figure above that the output power of PAT 2 is greater than the PAT no. 1 and 3 in the duration of 7–23 h. It is caused, similar to the first scenario, due to the increased flow rate and higher efficiency of PAT No. 2 in comparison to the other two PATs. Also, during the period of 1–6 h and 24 pm, the output power of PAT no. 1 is equal to zero, which is due to reversing the flow direction in pipe 4 (where PAT no. 1 is installed on it) and thus the installed PAT on this

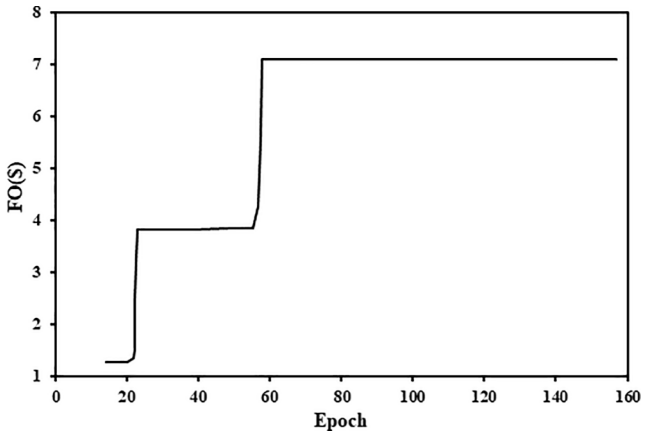

Fig. 10. The variation of Objective function with iteration in scenario 1.

Table 4
Characteristics of the PATs installed in the WDN in Scenario no. 1.

PAT number	Q_{BEP} (m^3/h)	H_{BEP} (m)
1	15.25	44.8
2	15.25	44.8
3	53.35	94.13

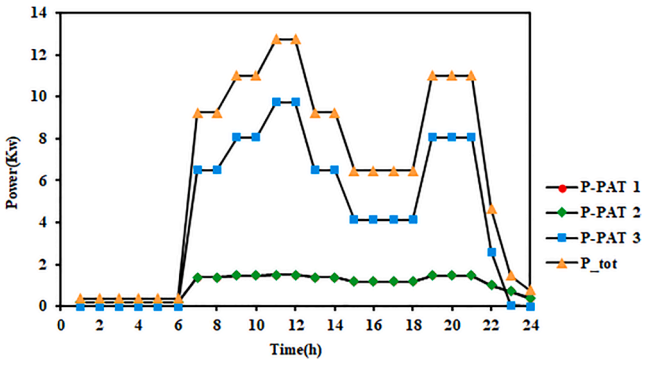

Fig. 11. The output power of each PAT and the total output power in Scenario no. 1.

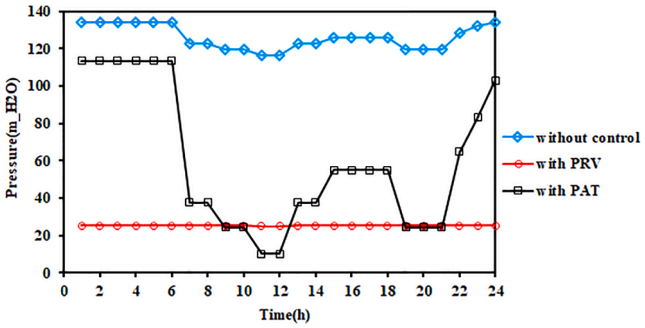

Fig. 12. Pressure of node 4 in Network No. 3 for three modes: Network with no PRV, Network with PRV, and Network with PATs.

pipe acted as a check valve causing the flow to be zero. Also, the output power of PAT 2 is very close to zero in the period of 1–6 h and 24 pm, which is due to that the working point of PAT 2 is very close to its runaway speed curve and its efficiency is very low. The same is true for PAT 3 during 1–6 h and 23–24 h. Figs. 16 and 17 illustrate the pressure diagrams of nodes 4 and 6 in uncontrolled network, network with PRV and network with using PATs.

As in the previous case, when the network consumption is high, the performance of PATs is close to the PRV, but with reduced network consumption at the early and late hours of the day, the PAT performance is diverged from the PRV and therefore the pressure of the nodes raises.

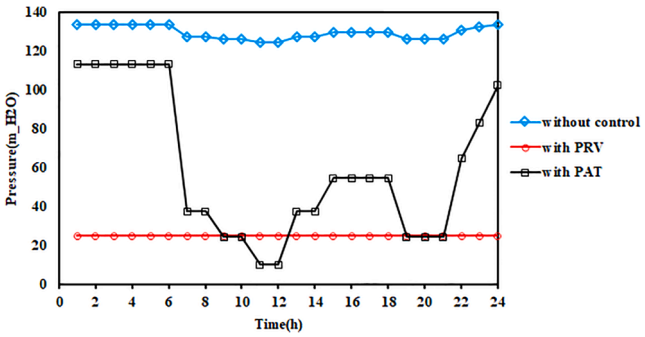

Fig. 13. Pressure of node 6 in Network No. 3 for three modes: Network without PRV, Network with PRV, and Network with PATs.

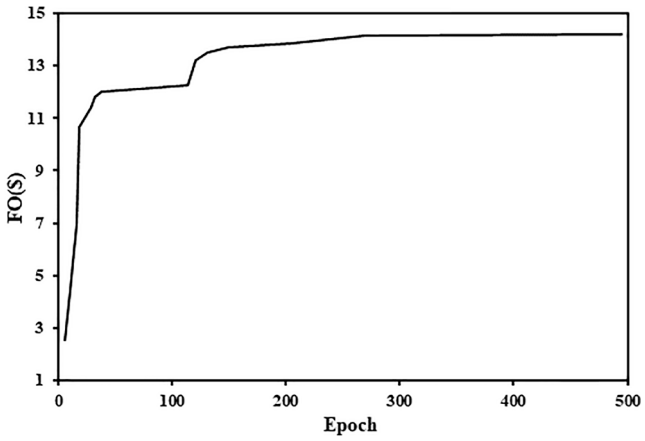

Fig. 14. Change in objective function in terms of iteration in scenario 2.

Table 5
Characteristics of the PATs installed in the WDN in Scenario no. 2.

PAT number	Q_{BEP} (m^3/h)	H_{BEP} (m)	Rotational speed (rpm)
1	15.2	30.6	2556
2	16.85	30.2	2441
3	26.75	57.4	1981

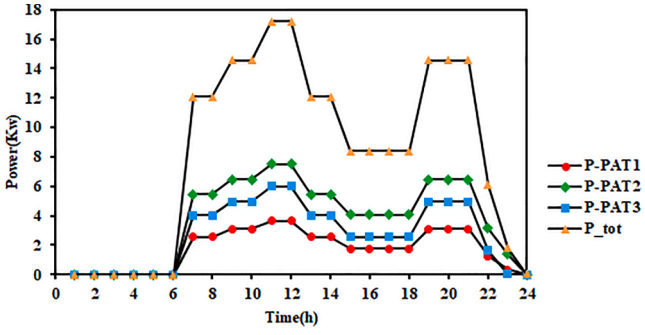

Fig. 15. The output power of each PAT and the total output power in Scenario no. 2.

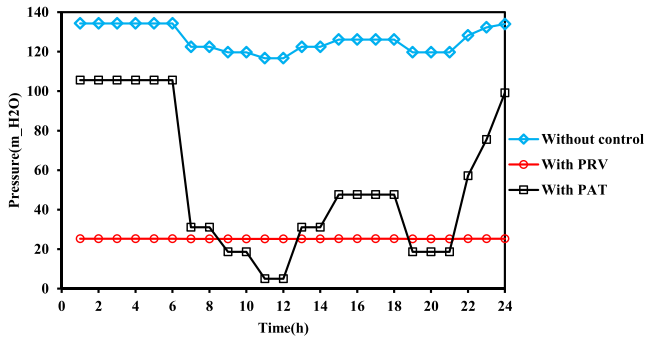

Fig. 16. Pressure of node 4 in Network No. 3 for three modes: Network with no PRV, Network with PRV, and Network with PATs obtained from the second stage of optimization process.

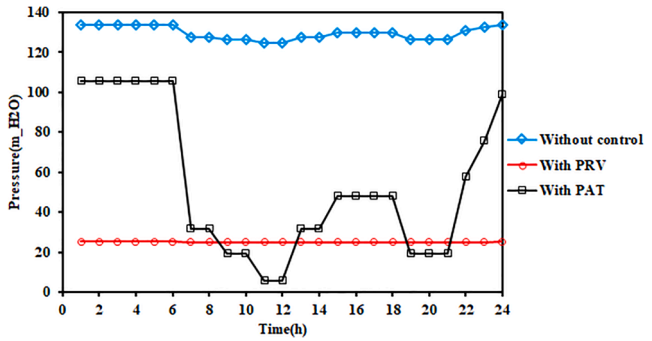

Fig. 17. Pressure of node 6 in Network No. 3 for three modes: Network with no PRV, Network with PRV, and Network with PATs obtained from the second stage of optimization process.

5.4. Scenario no. 3

In order to bring the pressure of the critical nodes in PAT utilization mode to as close as possible to the pressure while using PRV, the speed of the PATs must change over time. As with the previous two scenarios, the PSO algorithm is applied for optimization as well, and the only difference with the two previous scenarios is that the two PSO algorithms were nested. The head and flow rate of the optimal PATs in 1450 rpm were stated in Table 6.

The selected hourly rotational speeds for each of the PATs were also reported in Table 7. According to this table and the operating speed of PATs at different hours, it is determined that from 7 to 12 o'clock with increasing network consumption, PATs performance speeds decreases and then with decreasing the consumption, these values increase.

The total amount of energy produced over 24 h period is 182.15 kWh. By comparing the obtained values with the previous ones, it can be seen that the amount of harvested power compared to the scenario no. 1 was increased by 19.5% and decreased by 7.5%, compared to scenario no. 2. The amount of discharge leakage decreased by 26.6% and 10.1% in comparison with scenario no. 1 and 2, respectively. Also, the penalty function was decreased by 63.5% and 61.88% in comparison with scenario no. 1 and 2, respectively which indicates that the pressure of the critical nodes in this scenario is closer to those values of PRV utilization. Fig. 18 shows the power output of each of these PATs, as well as the total power generation within 24 h.

Table 6
Characteristics of the PATs installed in the WDN in Scenario no. 3.

PAT number	Q_{BEP} (m^3/h)	H_{BEP} (m)
1	26.75	57.4
2	15.25	44.8
3	45.1	46.3

Table 7
Rotational speed of PATs obtained from the third stage optimization at different hours.

Hour	Rotational speed of PAT 1 (rpm)	Rotational speed of PAT 2 (rpm)	Rotational speed of PAT 3 (rpm)
1–6	0	1385	1278
7–8 and 13–14	2272	2483	2479
9–10 and 21	2091	2282	2275
11–12	1872	2061	2058
15–18	2492	2710	2712
22	2582	2800	2800
23	0	2800	2800
24	0	1556	1548

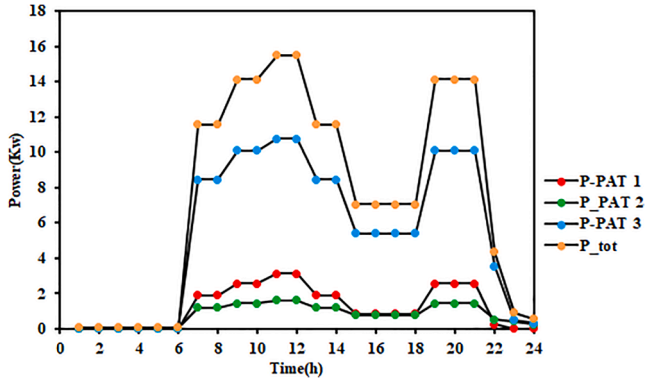

Fig. 18. The output power of each PAT and the total output power in Scenario no. 3.

From the above figure, it can be stated that the output of PAT n. 3 is higher than the other two PATs at all times, which is due to the higher discharge and efficiency of this PAT. Figs. 19 and 20 illustrate the pressure diagrams of nodes 4 and 6 over 24 h in three uncontrolled network, network with PRV and network with PAT.

In this case, in duration 7–22 h, the pressure of nodes 4 and 6 through PAT operating hours is approximately equal to the pressure of the network with PRV. Also, the pressure of the desired nodes has decreased significantly at 23 h compared to the previous scenarios and is very close to the pressure of the PRV mode, but as before, from 1 to 6 h and 24 pm the critical node pressure value When using PAT, higher than that of using PRV.

To better understand the use of variable speed PATs, Fig. 21

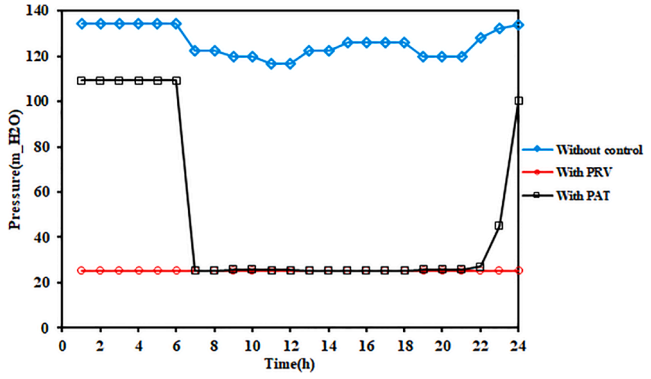

Fig. 19. Pressure of node 4 in Network No. 3 for three modes: Network with no PRV, Network with PRV, and Network with PATs obtained from the third stage of optimization process.

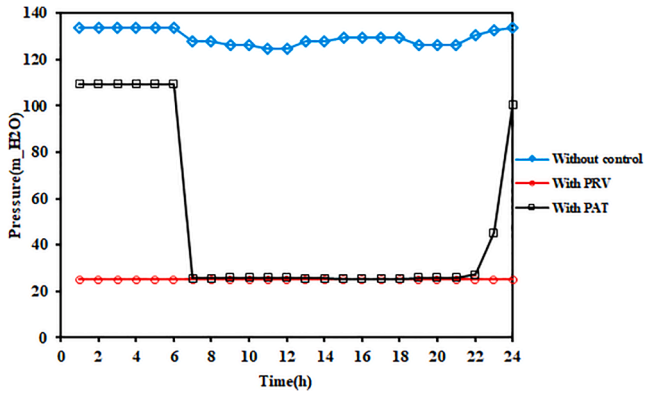

Fig. 20. Pressure of node 6 in Network No. 3 for three modes with no PRV, Network with PRV, and Network with PATs obtained from the third stage of optimization process.

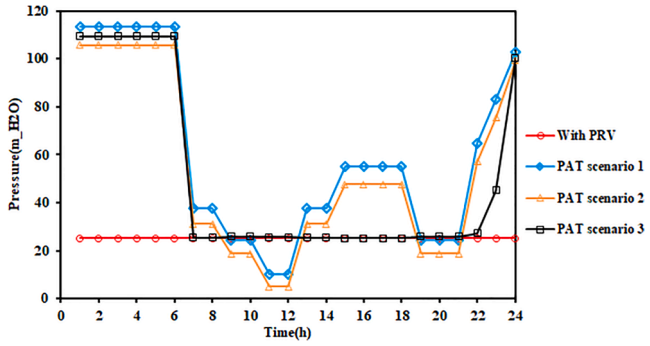

Fig. 21. Pressure of node 4 in Network No. 3 for four different modes.

demonstrates the pressure of node 4 in different states of PAT utilization as well as PRVs. It is illustrated in this figure that in the 7–22 period, PRV could be replaced by variable speed PAT without changing the pressure of critical nodes. But during the period of 1–6 h and 23–24 h, these PATs cannot perform well in place of PRVs.

If the combination of PRV and PAT is used in parallel, which means using PRV at 1–6 h and 23–24 h and PAT during 7–22 h, the pressure diagram of node 4 would be as plotted in Fig. 22:

6. Conclusion

This paper aimed to optimize PAT selection for replacement with PRVs in urban WDNs. To this end, the performance curves of PATs for the wide range of specific speeds were initially extracted considering the available performance data of pump manufactures. The optimization process was carried out for three scenarios. In the first scenario, the operating speeds of the selected PATs are the same and constant throughout the day, in the second scenario the speed of the selected PATs was considered to be different from each other, but constant throughout the day. According to the results of these two scenarios, when the network consumption is high, PATs can perform well and generate power in addition to controlling network pressure. However, at times when the network consumption was low, PAT performance dropped both in terms of network pressure control and power generation, and the pressure of critical nodes exceeded the desired standard. For this purpose, in the third optimization scenario, the operating speeds of PATs were considered to be variable. The results showed that the variation of the speed caused the amount of network produced energy to be reduced slightly compared to the second scenario, but the performance of the system in terms of pressure control was significantly improved except that in the start and end hours of the day. In order to

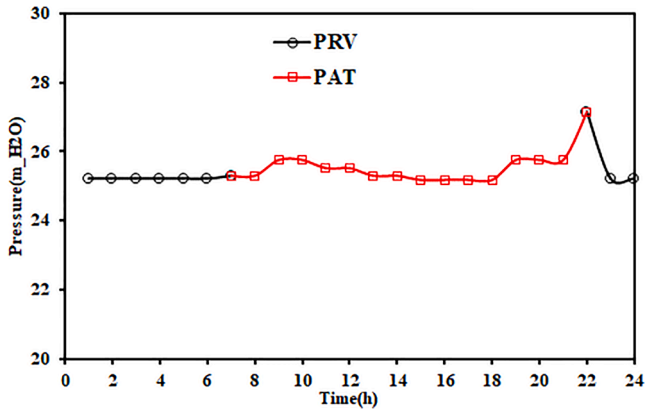

Fig. 22. Pressure of node 4 in Network No. 3 in parallel using of PRV and PAT.

keep the network pressure in the standard range at all hours of the day, the combination of PAT and PRV can be implied to generate the power in addition to adjusting the pressure. In this way, the PATs work only for hours when they can adjust the required standard pressure and for the rest of it, PRV regulates the pressure. In this case, in addition to control the pressure continuously, significant energy can be extracted from the network. It is worthy to note that the cost of maintenance and auxiliary equipment needed for speed variation have not been considered due to the lack of valid data. Future works can include implementation of optimized operation variable speed PAT in a real WDN that can be accompanied by significance fluctuations and disturbances in hydraulic parameters.

CRediT authorship contribution statement

Shahin Ebrahimi: Software, Resources, Investigation, Writing - original draft, Software, Validation. **Alireza Riasi:** Conceptualization, Methodology, Supervision. **Ali Kandi:** Writing - review & editing, Software.

Declaration of Competing Interest

The authors declare that they have no known competing financial interests or personal relationships that could have appeared to influence the work reported in this paper.

References

[1] Razmi A, Soltani M, Kashkooli FM, Garousi Farshi L. Energy and exergy analysis of an environmentally-friendly hybrid absorption/recompression refrigeration system. Energy Convers Manag 2018;164:59–69.
[2] Razmi A, Soltani M, Tayefeh M, Torabi M, Dusseault MB. Thermodynamic analysis of compressed air energy storage (CAES) hybridized with a multi-effect desalination (MED) system. Energy Convers Manag 2019;199:112047.
[3] Babaei SM, Razmi AR, Soltani M, Nathwani J. Quantifying the effect of nanoparticles addition to a hybrid absorption/recompression refrigeration cycle. J Clean Prod 2020;260:121084.
[4] Xu B, Chen D, Venkateshkumar M, Xiao Y, Yue Y, Xing Y, et al. Modeling a pumped storage hydropower integrated to a hybrid power system with solar-wind power and its stability analysis. Appl Energy 2019;248:446–62.
[5] Razmi AR, Janbaz M. Exergoeconomic assessment with reliability consideration of a green cogeneration system based on compressed air energy storage (CAES). Energy Convers Manag 2020;204:112320.
[6] Zeynalian M, Hajialirezaei AH, Razmi AR, Torabi M. Carbon dioxide capture from compressed air energy storage system. Appl Therm Eng 2020;178:115593.
[7] Soltani M, Nabat MH, Razmi AR, Dusseault M, Nathwani J. A comparative study between ORC and Kalina based waste heat recovery cycles applied to a green compressed air energy storage (CAES) system. Energy Convers Manag 2020;222:113203.
[8] Roushenas R, Razmi AR, Soltani M, Torabi M, Dusseault MB, Nathwani J. Thermo-environmental analysis of a novel cogeneration system based on solid oxide fuel cell (SOFC) and compressed air energy storage (CAES) coupled with turbocharger. Appl Therm Eng 2020;181:115978.

[9] Xu B, Li H, Campana Elia P, Hredzak B, Chen D. Dynamic regulation reliability of a pumped-storage power generating system: effects of wind power injection. Energy Convers Manag 2020;222:113226.
[10] Razmi AR, Arabkoohsar A, Nami H. Thermoeconomic analysis and multi-objective optimization of a novel hybrid absorption/recompression refrigeration system. Energy 2020;210:118559.
[11] Razmi A, Soltani M, Torabi M. Investigation of an efficient and environmentally-friendly CCHP system based on CAES, ORC and compression-absorption refrigeration cycle: energy and exergy analysis. Energy Convers Manag J 2019;195:1199–211.
[12] Binama M, Su W-T, Li X-B, Li F-C, Wei X-Z, An S. Investigation on pump as turbine (PAT) technical aspects for micro hydropower schemes: a state-of-the-art review. Renew Sustain Energy Rev 2017;79:148–79.
[13] Razmi A, Soltani M, Aghanajaf C, Torabi M. Thermodynamic and economic investigation of a novel integration of the absorption-recompression refrigeration system with compressed air energy storage (CAES). Energy Convers Manag 2019;187:262–73.
[14] Nourbakhsh S, Derakhshan E, Javidpour AR. Centrifugal & axial pumps used as turbines in small hydropower stations. Int. Congr. small hydropower, Lausanne, Switzerland. 2010.
[15] Nourbakhsh SA, Jahangiri G. Inexpensive small hydropower stations for small areas of developing countries. In: Conf. Adv. Planningt, Design Manag. Irrig. Syst. as Relat. to Sustain. L. use, louvain, Belgium; 1992. p. 14–7.
[16] Thoma D, Kittredge CP. Centrifugal pumps operated under abnormal conditions. Power 1931;73:881–4.
[17] Chapallaz JM, Eichenberger P, Fischer P. Manual on Pumps Used as Turbine. 1992.
[18] Páscoa JC, Silva FJ, Pinheiro JS, Martins DJ. Accuracy details in realistic CFD modeling of an industrial centrifugal pump in direct and reverse modes. J Therm Sci 2010;19:491–9.
[19] Derakhshan S, Nourbakhsh A. Experimental study of characteristic curves of centrifugal pumps working as turbines in different specific speeds. J Exp Therm Fluid Sci 2008;32:800–7.
[20] Derakhshan S, Nourbakhsh A. Theoretical, numerical and experimental investigation of centrifugal pumps in reverse operation. Exp Therm Fluid Sci 2008;32:1620–7.
[21] Barbarelli S, Amelio M, Florio G. Predictive model estimating the performances of centrifugal pumps used as turbines. Energy 2016;107:103–21.
[22] Barbarelli S, Amelio M, Florio G. Experimental activity at test rig validating correlations to select pumps running as turbines in microhydro plants. Energy Convers Manag 2017;149:781–97.
[23] Carravetta A, Del Giudice G, Fecarotta O, M. Ramos H.. Energy production in water distribution networks: a PAT design strategy. Water Resour Manag 2012;26:3947–59.
[24] Du J, Yang H, Shen Z, Chen J. Micro hydro power generation from water supply system in high rise buildings using pump as turbines. Energy 2017;137:431–40.
[25] Fontana N, Giugni M, Portolano D. In: Losses Reduction and Energy Production in water-distribution Networks; 2012. p. 237–44.
[26] Tahani M, Kandi A, Moghimi M, Derakhshan Houreh S. Rotational speed variation assessment of centrifugal pump-as-turbine as an energy utilization device under water distribution network condition. Energy 2020;213:118502.
[27] Lydon T, Coughlan P, McNabola A. Pressure management and energy recovery in water distribution networks: development of design and selection methodologies using three pump-as-turbine case studies. Renewable Energy 2017;114:1038–50.
[28] Lima GM, Luvizotto E, Brentan BM. Selection and location of Pumps as Turbines substituting pressure reducing valves. Renewable Energy 2017;109:392–405.
[29] Alberizzi JC, Renzi M, Righetti M, Roberto Pisaturo G, Rossi M. speed and pressure controls of pumps-as-turbines installed in branch of water-distribution network subjected to highly variable flow rates. Energies 2019;12:4738.
[30] Gulich JF. Centrifugal Pumps. Springer; 2010.
[31] Bhave PR. Analysis of Flow in Water Distribution Networks. Technomic Publishing Co; 1991.
[32] Brentan BM, Luvizotto Jr Edevar. Refining PSO applied to electric energy cost reduction in water pumping refining PSO applied to electric energy cost reduction in water pumping. Water Res Manag 2015;4:19–30.